ORGANOMETALLICS

Structural consequences of oxidation of ferrocene derivatives. 1. [0.0]Ferrocenophanium picrate hemihydroquinone

Manny Hillman, and Aabe Kvick

Organometallics, **1983**, 2 (12), 1780-1785• DOI: 10.1021/om50006a013 • Publication Date (Web): 01 May 2002

Organometallics is published by the American Chemical Society. 1155 Sixteenth Street N.W., Washington, DC 20036

portions of solvent. Total weight of solid material isolated in this manner was 0.145 g (53% yield): ESR (THF) $g = 1.98$, $a(^{31}P) = 19.5$ G (doublet), $a(^{91}Zr) = 13.5$ G (sextet). Anal. Calcd for $C_{23}H_{22}ZrP$: C, 65.68; H, 5.27; Zr, 21.69; P, 7.36; Cl, 0.00. Found: C, 60.30, 67.72; H, 4.91, 4.94; Zr, 20.30; P, 6.67; Cl, 1.95.

The magnetic susceptibility was estimated by preparing a 1% solution in benzene, which gave rise to an 8.5-Hz shift of the solvent resonance at 90 MHz. This gives rise to $\chi_g = (3.60 \pm 0.36) \times 10^{-6}$, $\chi_M = (1.51 \pm 0.15) \times 10^{-3}$, and $\mu_{eff} = 1.90 \pm 0.10$.

Acknowledgment. We wish to thank Professors R. G. Bergman, N. J. Cooper, and T. J. Marks for helpful discussions. We thank the Committee on Research of the University of California and the University of California at Davis NMR Facility for financial support. Purchase of the NT-200 and NT-360 instruments was made possible by an instrumentation grant from the National Science Foundation (Grant CHE-79-04832). Grateful acknowledgment is also made to the donors of the Petroleum Research Fund, administered by the American Chemical Society, for the support of this research.

Registry No. 1, 74380-49-7; 4, 74395-16-7; 7, 54634-14-9; 8, 87184-11-0; 11, 87184-10-9; 12, 74379-16-1; 15, 87184-09-6; 17, 87184-08-5.

Supplementary Material Available: Listings of atomic coordinates (Tables VI, XII, and XVIII), bond lengths (Tables VII, XIII, and XIX), bond angles (Tables VIII, XIV, and XX), temperature factors (Tables IX, XV, and XXI), derived hydrogen coordinates (Tables X, XVI, and XXII), and structure factors (Tables XI, XVII, and XXIII) for **4**, **12**, and **17** and a description of the determination of D/H distribution in "$(C_5D_5)_2ZrCl$" (79 pages). Ordering information is given on any current masthead page.

Structural Consequences of Oxidation of Ferrocene Derivatives. 1. [0.0]Ferrocenophanium Picrate Hemihydroquinone

Manny Hillman*[†] and Åbe Kvick[‡]

Chemical Sciences Division, Department of Energy and Environment, and Department of Chemistry, Brookhaven National Laboratory, Upton, New York 11973

Received August 1, 1983

The crystal and molecular structures of the title compound I, $C_{20}H_{16}Fe_2^{+}\cdot C_6H_2N_3O_7^{-}\cdot {}^1/_2(C_6H_6O_2)$, were determined. The plane of the picrate lies essentially parallel to the planes of the cyclopentadienyl rings of the ferrocenophane with indication of some degree of charge transfer. The hydroquinone is hydrogen bonded to the O(1) oxygen atoms of two picrates and lies essentially normal to the picrate and to the ferrocenophane separating two-dimensional layers of picrate–ferrocenophane stacks. The iron–iron distance is 363.6 (1) pm, 34 (2) pm shorter than in the neutral ferrocenophane, supporting a theory that the average valency of this ferrocenophane monocation is due at least partially to an iron–iron interaction and not exclusively to an interaction through the cyclopentadienyl rings.

Introduction

The preparation[1-5] of [0.0]ferrocenophane (II) and the subsequent preparation of its mono-[2-5] and dications[5,6] have led to an extensive investigation of the physical properties of these compounds, both experimentally[1-13] and theoretically.[14] Of principal concern were questions on the interaction between the iron atoms and on the average or mixed valency of the monocation. The results[15] of the crystal and molecular structure of II excluded the likelihood of an iron–iron interaction in that compound. The observed iron–iron distance in II of 398 (2) pm is 6 pm longer than that expected from perfectly aligned cyclopentadienyl rings with the iron atoms on the axes normal to the centroids of those rings. A very small repulsion is all that can be discerned. On the other hand, the observation that the monocation is average valent, by virtue of the identical irons observed in both Mössbauer[3,5,8,10] and ESCA[3,5,13] measurements, requires a strong iron–iron interaction. The interaction may be directly between the irons[8,9,11,12] or through the cyclopentadienyl rings[5-7,10,14] or by both paths. These unreconciled theories prompted the present work: the determination of the crystal structure of the monocation, as exemplified by the title compound, I.

Table I. Crystal Data

mol formula	$C_{20}H_{16}Fe_2\cdot C_6H_2N_3O_7\cdot {}^1/_2(C_6H_6O_2)$
mol wt	651.14
space group	$P\bar{1}$
a, pm	1039.9 (1)
b, pm	1374.8 (4)
c, pm	1022.5 (1)
α, deg	91.01 (2)
β, deg	118.99 (1)
γ, deg	78.23 (1)
V, nm^3	1.2462
Z	2
ρ_{calcd} g/cm^3	1.770
abs coeff, cm^{-1}	11.89
2θ range, deg	2–60
reflctns used ($F > 3\sigma$)	8025
parameters refined	5245
scan width	463
$R(F) = \Sigma\|F_o - F_c\|/\Sigma\|F_o\|$	$0.75 + 0.35 \tan\theta$
$R_w(F) = \Sigma\|F_o - F_c\|w^{1/2}/$	0.039
$\Sigma\|F_o\|w^{1/2}$ ($w = 1/(\sigma^2(F) +$	0.038
$0.0005F^2$))	0.07
max shift/error (non-H)	0.12
max shift/error (H)	510
residual electron density, e nm^{-3}	

[†] Chemical Sciences Division, Department of Energy and Environment.

[‡] Department of Chemistry.

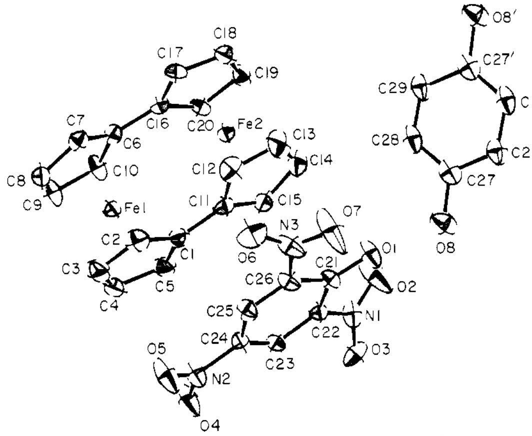

Figure 1. ORTEP diagram showing the non-hydrogen atoms of the three molecular moieties with 50% thermal ellipsoids.

Experimental Section

The neutral compound, II, was prepared by the Cowan and LeVanda[3] modification of the procedure of Hedberg and Rosenberg.[1] Compound I was prepared by a modification of the procedure in the literature.[4] CH_2Cl_2 was used in place of benzene as a solvent. In one experiment, where the ratios of II to picrate to quinone were 1.0:5.4:2.9, respectively, and II appeared to be dissolved in the solvent before addition of the other reactants, slow evaporation of the solvent yielded sizable, dark, bluish green crystals. One, measuring approximately 0.4 × 0.25 × 0.2 mm, mounted along the long axis, was used for the collection of diffraction intensity data.

The intensity data were collected on an Enraf-Nonius CAD-4 diffractometer with graphite-monochromated Mo Kα radiation (λ = 71.07 pm). The diffraction symmetry was determined to be triclinic from preliminary film data, and the centrosymmetric form was established from the success of the refinement. The unit cell dimensions (Table I) were determined from 25 reflections with $32° < 2\theta < 48°$. Intensities were collected by using θ-2θ scans and were not corrected for Lorentz and polarization effects. No absorption correction was performed (μ = 11.89 cm^{-1}).

The structure was determined by using the SHELX-76 crystallographic computing package.[16] The atomic scattering factors for iron including components for anomalous dispersion were taken from tabulations of Doyle and Turner[17] and Cromer and Liberman.[18] Those for hydrogen are from Stewart et al.[19] The other atomic scattering factors are from Cromer and Mann.[20] The iron

Table II. Fractional Coordinates[a] of Non-Hydrogen Atoms

atom	x	y	z
Fe1	46 767 (3)	22 529 (2)	45 899 (3)
Fe2	29 262 (3)	17 084 (2)	67 433 (3)
C1	56 185 (25)	24 222 (18)	68 846 (25)
C2	51 856 (31)	33 546 (19)	60 188 (30)
C3	60 082 (34)	32 693 (23)	52 222 (33)
C4	69 123 (29)	22 914 (24)	55 590 (32)
C5	66 741 (25)	17 602 (20)	65 706 (27)
C6	26 516 (22)	17 877 (15)	35 902 (22)
C7	24 801 (25)	27 288 (16)	28 786 (24)
C8	34 926 (28)	26 010 (18)	22 982 (25)
C9	43 112 (27)	15 915 (18)	26 604 (25)
C10	38 095 (25)	10 865 (16)	34 692 (23)
C11	49 715 (25)	21 588 (18)	77 663 (24)
C12	38 641 (28)	28 186 (18)	80 087 (26)
C13	33 833 (31)	22 572 (22)	87 680 (29)
C14	41 703 (31)	12 541 (22)	89 993 (28)
C15	51 479 (27)	11 820 (19)	83 727 (25)
C16	19 149 (22)	16 145 (16)	44 270 (23)
C17	10 118 (24)	23 710 (17)	48 072 (26)
C18	6 332 (27)	19 084 (20)	57 627 (29)
C19	13 027 (30)	8 817 (20)	59 976 (31)
C20	21 146 (28)	6 880 (17)	51 924 (28)
C21	93 031 (24)	28 966 (16)	92 857 (24)
C22	95 979 (23)	19 145 (16)	100 134 (23)
C23	89 968 (23)	17 052 (16)	108 811 (23)
C24	79 944 (25)	24 568 (17)	110 549 (25)
C25	75 720 (25)	34 046 (16)	103 357 (25)
C26	81 892 (26)	36 078 (15)	94 932 (25)
C27	5 352 (28)	47 852 (17)	−34 685 (28)
C28	−8 415 (28)	45 974 (17)	−45 283 (31)
C29	−13 742 (27)	48 019 (17)	−60 442 (29)
N1	106 146 (22)	10 837 (14)	98 613 (24)
N2	73 425 (24)	22 492 (17)	119 508 (24)
N3	76 105 (29)	46 059 (15)	87 063 (25)
O1	99 294 (21)	30 862 (13)	85 742 (21)
O2	106 632 (31)	10 646 (15)	86 909 (28)
O3	113 443 (18)	4 075 (13)	108 939 (21)
O4	76 402 (26)	13 834 (15)	124 870 (26)
O5	65 246 (27)	29 312 (16)	121 610 (27)
O6	63 374 (25)	50 481 (15)	84 130 (26)
O7	83 928 (34)	49 671 (16)	83 683 (36)
O8	11 266 (22)	45 901 (14(	−19 520 (21)

[a] The fractional coordinates are multiplied by 10^5.

Table III. Fractional Coordinates[a] of Hydrogen Atoms

atoms	x	y	z
H2	446 (2)	390 (2)	598 (3)
H3	592 (3)	375 (2)	453 (3)
H4	754 (3)	204 (2)	507 (3)
H5	714 (3)	107 (2)	700 (3)
H7	183 (2)	330 (2)	281 (2)
H8	368 (3)	310 (2)	181 (3)
H9	507 (3)	128 (2)	246 (3)
H10	415 (3)	40 (2)	385 (3)
H12	353 (3)	349 (2)	776 (3)
H13	265 (3)	253 (2)	903 (3)
H14	402 (4)	67 (2)	939 (4)
H15	586 (3)	60 (2)	836 (3)
H17	77 (3)	306 (2)	451 (3)
H18	6 (3)	227 (2)	627 (3)
H19	129 (3)	41 (2)	664 (3)
H20	265 (3)	8 (2)	514 (3)
H23	917 (3)	108 (2)	1128 (3)
H25	693 (2)	387 (2)	1044 (2)
H28	−136 (3)	429 (2)	−422 (3)
H29	−230 (2)	465 (2)	−682 (2)
HO8	69 (4)	423 (3)	−180 (4)

[a] The fractional coordinates are multiplied by 10^3.

---

(1) Hedberg, F. L.; Rosenberg, H. *J. Am. Chem. Soc.* **1969**, *91*, 1258–1259.

(2) Rausch, M. D.; Kovar, R. F.; Kraihanzel, C. S. *J. Am. Chem. Soc.* **1969**, *91*, 1259–1261.

(3) Cowan, D. O.; LeVanda, C. *J. Am. Chem. Soc.* **1972**, *94*, 9271–9272.

(4) Mueller-Westerhoff, U. T.; Eilbracht, P. *J. Am. Chem. Soc.* **1972**, *94*, 9272–9274.

(5) LeVanda, C.; Bechgaard, K.; Cowan, D. O.; Mueller-Westerhoff, U. T.; Eilbracht, P.; Candela, G. A.; Collins, R. L. *J. Am. Chem. Soc.* **1976**, *98*, 3181–3187.

(6) Mueller-Westerhoff, U. T.; Eilbracht, P. *Tetrahedron Lett.* **1973**, 1855–1858.

(7) LeVanda, C.; Bechgaard, K.; Cowan, D. O. *J. Org. Chem.* **1976**, *41*, 2700–2704.

(8) Morrison, W. H., Jr.; Hendrickson, D. N. *Chem. Phys. Lett.* **1973**, *22*, 119–123.

(9) Morrison, W. H., Jr.; Hendrickson, D. N. *Inorg. Chem.* **1974**, *13*, 2279–2280.

(10) Cowan, D. O.; LeVanda, C.; Collins, R.; Candela, G. A.; Mueller-Westerhoff, U. T.; Eilbracht, P. *J. Chem. Soc., Chem. Commun.* **1973**, 329–330.

(11) Morrison, W. H., Jr.; Krogsrud, S.; Hendrickson, D. N. *Inorg. Chem.* **1973**, *12*, 1998–2004.

(12) Morrison, W. N., Jr.; Hendrickson, D. N. *Inorg. Chem.* **1975**, *14*, 2331–2346.

(13) Boehm, M. C.; Gleiter, R.; Delgado-Pena, F.; Cowan, D. O. *Inorg. Chem.* **1980**, *19*, 1081–1082.

(14) Kirchner, R. F.; Loew, G. H.; Mueller-Westerhoff, U. T. *Inorg. Chem.* **1976**, *15*, 2665–2670.

(15) Churchill, M. R.; Wormald, J. *Inorg. Chem.* **1969**, *8*, 1970–1974.

(16) Sheldrick, G. M. In "Computing in Crystallography"; Schenk, H., Olthof-Hazekamp, R., van Koningsveld, H., Bassi, G. C., Eds.; Delft University Press: Delft, 1978; pp 34–42.

(17) Doyle, P. A.; Turner, P. S. *Acta Crystallogr., Sect. A* **1968**, *A24*, 390–397.

(18) Cromer, D. T.; Liberman, D. *J. Chem. Phys.* **1970**, *53*, 1891–1898.

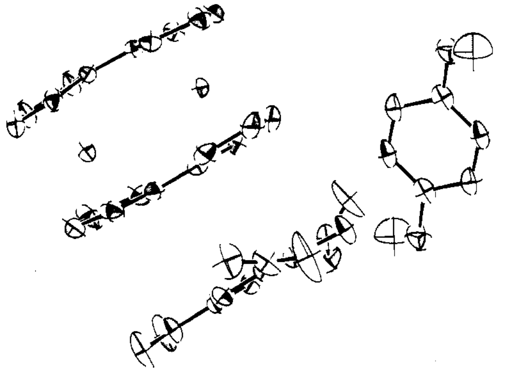

Figure 2. ORTEP diagram showing the three molecular moieties with 50% thermal ellipsoids. This view demonstrates the almost-parallel rings and the ring tilts in the ferrocenophane. The hydrogen bonds are shown.

atoms were located on Patterson maps, and the remaining atomic positions were obtained from successive difference Fourier maps. At the outset the structure was believed to contain only picrate and ferrocenophane. Least-squares refinement, however, did not reduce the $R(F)$ value below 0.17. The residual electron density map revealed four peaks with electron densities close to those expected for carbon atoms clustered around a center of symmetry. With the four symmetry related atoms, the arrangement of the eight atoms resembled the structure of a quinone molecule. (Since quinone was the agent used to oxidize II, this was not totally surprising.) Incorporation of the four atoms in the refinement lowered the $R(F)$ value close to the final value. The hydrogen atoms were then all located on a difference map, and it was determined that the "quinone" molecule was hydroquinone. Least-squares refinement of the coordinates of the non-hydrogen atoms with anisotropic thermal parameters and of the hydrogen atoms with isotropic thermal parameters was then done alternately until the shifts in the parameters were 0.1 of the estimated standard deviations or less. The final $R(F)$ was 0.038 for 463 variables and 5245 reflections. The largest remaining peak was near an iron atom and had an electron density of 510 e nm^{-3} as compared to 6000 e nm^{-3} for a typical carbon atom.

Results

The crystallographic data are summarized in Table I. The atomic coordinates are given in Tables II and III. The thermal factors and the observed and calculated structure factors are available as supplementary material. ORTEP diagrams of two views of the non-hydrogen atoms of the three molecules are given in Figures 1 and 2. The numbering scheme used is summarized in Figure 1. The stereo packing diagram in Figure 3 illustrates the one-dimensional stacking of the picrate and the ferrocenophane units and the two-dimensional layers of picrate/ferrocenophane and of hydroquinone. The hydrogen atoms involved in hydrogen bonding are included in the hydroquinone in Figures 2 and 3. Selected bond distances and angles are given in Tables IV and V. The least-squares planes of all of the rings and the dihedral angles between all pairs of planes are presented in Table VI.

Discussion

The investigation of the structural consequences of the oxidation of ferrocene derivatives has been essentially confined to ferrocenium salts with various anions,[21-27] to the triiodide of 1,1′-dimethylferrocenium,[28] and to the perchlorate of 1,1′,2,2′,4,4′-tris(trimethylene)ferrocenium.[29] The conclusion reached from these studies was that oxidation is accompanied by a lengthening of the distance between the iron and the plane of the ring by about 4–5 pm, possibly due to a weakening of the iron-to-ring in-

Table IV. Selected Bond Distances (pm)

Interunit Distances			
Fe1-Fe2	363.6 (1)		
C1-C11	144.8 (4)		
C6-C16	144.7 (4)		
unit 1		unit 2	
Fe1-C1	208.9 (2)	Fe2-C11	208.8 (2)
Fe1-C2	205.2 (3)	Fe2-C12	206.6 (2)
Fe1-C3	204.4 (4)	Fe2-C13	205.4 (3)
Fe1-C4	205.1 (3)	Fe2-C14	205.3 (2)
Fe1-C5	206.7 (2)	Fe2-C15	206.6 (2)
Fe1-C6	208.0 (2)	Fe2-C16	208.9 (2)
Fe1-C7	206.5 (2)	Fe2-C17	205.3 (2)
Fe1-C8	205.9 (2)	Fe2-C18	204.7 (3)
Fe1-C9	205.3 (3)	Fe2-C19	205.6 (3)
Fe1-C10	205.5 (2)	Fe2-C20	207.4 (2)
C1-C2	143.1 (4)	C11-C12	143.3 (4)
C2-C3	142.8 (6)	C12-C13	141.5 (5)
C3-C4	141.3 (4)	C13-C14	141.1 (4)
C4-C5	141.9 (5)	C14-C15	142.9 (5)
C5-C1	143.5 (4)	C15-C11	142.8 (4)
C6-C7	143.1 (3)	C16-C17	143.4 (4)
C7-C8	142.1 (5)	C17-C18	141.8 (5)
C8-C9	142.1 (3)	C18-C19	140.8 (4)
C9-C10	142.3 (4)	C19-C20	142.7 (5)
C10-C6	143.6 (3)	C20-C16	143.1 (4)
C2-H2	94 (3)	C12-H12	92 (2)
C3-H3	93 (3)	C13-H13	94 (4)
C4-H4	101 (4)	C14-H14	97 (4)
C5-H5	98 (2)	C15-H15	97 (3)
C7-H7	90 (2)	C17-H17	95 (2)
C8-H8	96 (3)	C18-H18	102 (3)
C9-H9	93 (3)	C19-H19	94 (3)
C10-H10	96 (2)	C20-H20	92 (3)
Picrate			
C21-C22	145.5 (3)	N1-O2	122.2 (4)
C22-C23	137.1 (4)	N1-O3	123.5 (3)
C23-C24	138.6 (3)	N2-O4	123.3 (3)
C24-C25	138.5 (3)	N2-O5	122.2 (4)
C25-C26	136.0 (5)	N3-O6	122.7 (4)
C26-C21	145.3 (4)	N3-O7	121.3 (5)
C21-O1	124.8 (4)	C23-H23	91 (3)
C22-N1	145.2 (3)	C25-H25	87 (2)
C24-N2	143.9 (4)		
C26-N3	145.8 (3)		
Hydroquinone			
C27-C28	138.8 (3)	C28-H28	91 (3)
C28-C29	138.1 (4)	C29-H29	97 (2)
C29-C27′	140.2 (2)	O8-HO8	81 (5)
C27-O8	137.0 (3)		
Hydrogen Bond			
HO8-O1	202 (4)	O1-O8	280.2 (3)
HO8-O7	248 (4)	O7-O8	295.9 (4)

---

(19) Stewart, R. F.; Davidson, E. H.; Simpson, W. T. *J. Chem. Phys.* **1965**, *42*, 3175–3187.

(20) Cromer, D. T.; Mann, J. B. *Acta Crystallogr., Sect. A* **1965**, *A24*, 321–325.

(21) Pettersen, R. C. Ph.D. Thesis, Univ. of Calif., Berkeley, Calif., 1966.

(22) Bernstein, T.; Herbstein, F. H. *Acta Crystallogr., Sect. B* **1968**, *B24*, 1640–1645.

(23) Landers, A. G.; Lynch, M. W.; Raaberg, S. B.; Rheingold, A. L.; Lewis, J. E. *J. Chem. Soc., Chem. Commun.* **1976**, 931–932.

(24) Mammano, J. J.; Zalkin, A.; Landers, A.; Rheingold, A. L. *Inorg. Chem.* **1977**, *16*, 297–300.

(25) Paulus, E. F.; Shaefer, L. *J. Organomet. Chem.* **1978**, *144*, 205–213.

(26) Rheingold, A. L.; Landers, A. G.; Dahlstrom, P.; Zubieta, J. *J. Chem. Soc., Chem. Commun.* **1979**, 143–144.

(27) Churchill, M. R.; Landers, A. G.; Rheingold, A. L. *Inorg. Chem.* **1981**, *20*, 849–853.

(28) Bats, J. W.; de Boer, J. J. *Inorg. Chim. Acta* **1971**, *5*, 605–610.

(29) Hillman, M.; Larson, A. C., unpublished results.

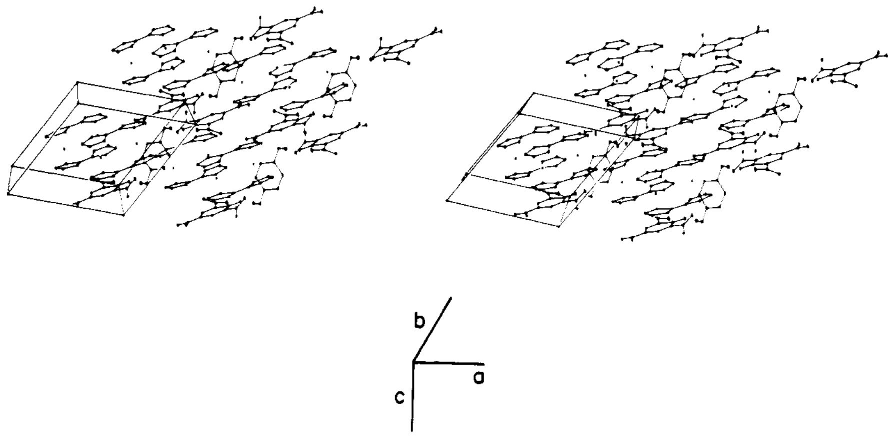

Figure 3. ORTEP packing diagram illustrating the stacking of the ferrocenophanes and the picrates. The hydrogen atoms involved in hydrogen bonding are shown. The ellipsoids are the smallest that are possible with ORTEP.

teraction. In I, as a consequence of the average valency, the charge is distributed uniformly over both ferrocene units. The expansion of the iron-to-ring distances is consequently expected to be the same for both ferrocene units. Since the charge on each ferrocene unit is $^{1}/_{2}+$, the iron-to-ring distances are expected to be lengthened by about half that observed in simple ferrocenium derivatives. These expectations have now been confirmed. In one ferrocene unit, the iron to ring distance is 166.7 (2) pm, and in the other unit it is 167.2 (2) pm, essentially the same and on the average 2.1 pm longer than the iron to ring distances reported for compound II.

Thus, the present structure provides an independent indication that the iron atoms in I are identical, confirming the ESCA and Mössbauer results mentioned earlier. The major remaining question concerns the nature of the interaction that distributes the electrons between both ferrocene units. There are two schools of thought. One[8,9,11,12] favors a direct iron–iron interaction, and the other[5–7] favors an interaction through the rings.

The rationale for the direct iron–iron interaction is as follows: ESR and magnetic susceptibility studies of the monocation support the delocalization of e_{2g} electrons over the two irons.[8] The large quadrupole splitting and the negative gradient of the quadrupole splitting of the dication also support the same kind of delocalization.[8,9] If the mechanism is by superexchange, i.e., through the cyclopentadienyl rings, then such exchange should also operate in the monocation of biferrocene, but this is not the case since that monocation is not average valent.[11] (Several monocations of biferrocene derivatives, however, have been found to be average valent: 1′,1‴-diiodo-,[12] 1′,1‴-diethyl-,[30] and 1′,1‴-dipropylbiferrocene[30,31] and (*as*-indacene)bis(cyclopentadienyliron).[32]) Furthermore, the contention is that the direction and extent of the iron orbitals in I and II are such that direct overlap is possible even at a distance of 398 pm.[12] The dication of II is diamagnetic, indicating a strong iron–iron interaction in that compound. This finds support in the dication of a [1.1]ferrocenophane, where interaction through the rings is insulated by methylene groups. It is diamagnetic even though the iron atoms of the neutral compound are 460 pm apart.[8,11,12]

It has been stated that the rationale for the interaction through the rings is as follows: The 398-pm distance between the irons in II is too long for direct overlap.[5,6] The [1.1]ferrocenophane can have a conformation with an iron–iron distance that is the same length, but the monocation is not average valent.[5] The diamagnetism of the dication of II can be caused by an interaction through the rings.[5,6] The monocation of a ferrocenophane with the ferrocene units separated by two ethynediyl units is average valent. In this compound the iron–iron distance is over 600 pm. The interaction can only be through the rings and the ethynediyl groups.[5,7]

Molecular orbital calculations[14] appear to favor the direct iron–iron interaction. The best agreement with the experimental Mössbauer data was obtained by removal of an electron from an antibonding orbital between the two iron atoms of II, indicating an increase in bonding of the irons in I, the oxidized form of II. The molecular orbital calculations, however, were based on the assumption of identical geometry for I and II, which is not correct. However, it was the only assumption that could be made at the time.

When compound II was first prepared,[1] consideration was given to the possibility that there might be a repulsion between the iron atoms, perhaps even to the extent that the bonding to the cyclopentadienyl rings would no longer be η^5. The determination[15] of its structure by X-ray crystallography, however, demonstrated that the repulsion, if present, was only minor. The iron atoms were 6 pm further apart than expected, and this was accommodated by a 2.3° tilt of the rings of each ferrocene unit with the opening of the tilt away from the centroid of the molecule.

Compound I has now been found to have an iron–iron distance of 363.6 (1) pm, 34 (2) pm shorter than in II. This apparent attraction of the iron atoms is accommodated by ring tilts of 9.6° in one ferrocene unit and 10.4° in the other unit with the opening of the tilts toward the centroid of the molecule, the reverse of that found in II (see Figure 2). The iron–iron attraction is also accommodated by C–C bonds joining the cyclopentadienyl rings (C1–C11 and C6–C16) that are shorter than those in II by 3 pm. All other bond lengths and angles in I are closely similar to those in II.

The short iron–iron distance is indicative of a direct iron–iron interaction. It does not, however, show that such an interaction is an exclusive explanation of the average valency of I, and some interaction through the rings is probably still important. For example, as obvious from the crystal structure of the 1′,1‴-dipropylbiferrocene monocation,[31] the average valency here must arise from an interaction through the rings. A fuller understanding of the interactions in I may now be obtainable by an im-

---

(30) Iijima, S.; Saida, R.; Motoyama, I.; Sano, H. *Bull. Chem. Soc. Jpn.* **1981**, *54*, 1375–1379.

(31) Konno, M.; Hyodo, S.; Iijima, S. *Bull. Chem. Soc. Jpn.* **1982**, *55*, 2327–2335.

(32) Iijima, S.; Motoyama, I.; Sano, H. *Bull. Chem. Soc. Jpn.* **1980**, *53*, 3180–3183.

Table V. Selected Bond Angles (deg)

Ferrocenophane			
unit I		unit II	
C1-C2-C3	107.8 (2)	C11-C12-C13	108.4 (2)
C2-C3-C4	108.3 (3)	C12-C13-C14	108.2 (3)
C3-C4-C5	108.4 (3)	C13-C14-C15	108.4 (3)
C4-C5-C1	108.1 (2)	C14-C15-C11	107.8 (2)
C5-C1-C2	107.3 (3)	C15-C11-C12	107.2 (3)
C6-C7-C8	108.1 (2)	C16-C17-C18	108.1 (2)
C7-C8-C9	108.3 (3)	C17-C18-C19	108.2 (3)
C8-C9-C10	108.2 (3)	C18-C19-C20	108.7 (3)
C9-C10-C6	108.0 (2)	C19-C20-C16	107.5 (2)
C10-C6-C7	107.4 (2)	C20-C16-C17	107.5 (3)
C1-C2-H2	124 (2)	C11-C12-H12	127 (2)
C3-C2-H2	128 (2)	C13-C12-H12	125 (2)
C2-C3-H3	127 (2)	C12-C13-H13	124 (2)
C4-C3-H3	125 (2)	C14-C13-H13	128 (2)
C3-C4-H4	122 (2)	C13-C14-H14	128 (2)
C5-C4-H4	129 (2)	C15-C14-H14	123 (2)
C4-C5-H5	127 (2)	C14-C15-H15	130 (2)
C1-C5-H5	125 (2)	C11-C15-H15	123 (2)
C5-C1-C11	126.2 (2)	C15-C11-C1	126.8 (2)
C2-C1-C11	126.1 (2)	C12-C11-C1	125.4 (2)
C6-C7-H7	125 (2)	C16-C17-H17	125 (2)
C8-C7-H7	127 (2)	C18-C17-H17	127 (2)
C7-C8-H8	128 (2)	C17-C18-H18	125 (2)
C9-C8-H8	124 (2)	C19-C18-H18	126 (2)
C8-C9-H9	129 (2)	C18-C19-H19	126 (2)
C10-C9-H9	123 (2)	C20-C19-H19	125 (2)
C9-C10-H10	127 (2)	C19-C20-H20	127 (2)
C6-C10-H10	125 (2)	C16-C20-H20	126 (2)
C7-C6-C16	125.6 (2)	C17-C16-C6	125.6 (2)
C10-C6-C16	126.6 (2)	C20-C16-C6	126.4 (2)
Picrate			
C21-C22-C23	124.5 (2)	C24-C25-H25	120 (2)
C22-C23-C24	119.2 (2)	C26-C25-H25	121 (2)
C23-C24-C25	120.7 (3)	C25-C26-N3	115.7 (2)
C24-C25-C26	119.6 (2)	C21-C26-N3	119.5 (3)
C25-C26-C21	124.8 (2)	C22-N1-O2	118.5 (2)
C26-C21-C22	111.0 (2)	C22-N1-O3	118.6 (3)
C22-C21-O1	123.6 (2)	O2-N1-O3	122.9 (2)
C26-C21-O1	125.4 (2)	C24-N2-O4	118.4 (3)
C21-C22-N1	119.5 (3)	C24-N2-O5	119.3 (2)
C23-C22-N1	116.0 (2)	O4-N2-O5	122.3 (3)
C22-C23-H23	122 (2)	C26-N3-O6	118.0 (3)
C24-C23-H23	119 (2)	C26-N3-O7	119.4 (3)
C23-C24-N2	120.0 (2)	O6-N3-O7	122.6 (2)
C25-C24-N2	119.2 (2)		
Hydroquinone			
C29′-C27-C28	119.1 (4)	C27-C28-H28	119 (1)
C27-C28-C29	120.7 (3)	C29-C28-H28	120 (1)
C28-C29-C27′	120.2 (5)	C28-C29-H29	123 (2)
C29′-C27-O8	117.6 (4)	C27′-C29-H29	117 (2)
C28-C27-O8	123.3 (3)	C27-O8-HO8	110 (2)
Hydrogen Bond			
O1-HO8-O8	168 (4)	O7-HO8-O8	119 (3)

proved molecular orbital calculation using the experimental geometry of the molecule.

We are aware of one other example[33] of an average valent monocation, $[\mathrm{Fe}(\eta^5\text{-}\mathrm{C}_5\mathrm{H}_5)(\mathrm{CO})(\mathrm{SCH}_3)]_2$, where the iron–iron distance is 46 pm shorter than in the neutral parent compound. It has been proposed that the shortening of the iron–iron distance is due to the removal of an electron from an antibonding orbital between the two irons[34,35] in accord with the calculations for the ferrocenophane monocation.[14] In an average valent molybdenum monocation,[36] $[\mathrm{Mo}(\eta^5\text{-}\mathrm{C}_5\mathrm{H}_5)(\mathrm{SCH}_3)_2]_2$, however, the intermetal distance is 1.4 pm longer than in the neutral parent compound. In the latter case, the failure to produce a shorter distance can be attributed to the removal of a nonbonding electron.

The arrangement of the different molecules in the crystal lattice suggests the possibility of π-orbital interaction and linear charge transfer between the picrate and the ferrocenophane molecules. Each picrate ring is approximately parallel to the rings of one ferrocenophane and positioned 325 pm from the average plane of the nearest pair of cyclopentadienyl rings and coming very close to eclipsing them (see Figure 2). These closely associated pairs of molecules are stacked through the crystal lattice (Figure 3), with successive pairs displaced by less than the width of one picrate molecule. This type of arrangement, alternation of picrate, ferrocenophane, picrate, etc., however, is associated with low conductivity. Indeed, the conductivity of I (though probably without the hydroquinone in the crystal) has been reported[37] to be $10^{-7}\ \Omega^{-1}\ \mathrm{cm}^{-1}$, while that[4] of the tetracyanoquinodimethane (TCNQ) salt of ferrocenophane is $>10\ \Omega^{-1}\ \mathrm{cm}^{-1}$.

It is also of interest to note that in this compound the cyclopentadienyl rings of the ferrocenophane are parallel to a planar aromatic compound. There appears to be no universality to this arrangement. In ferrocenium picrate[21] the cyclopentadienyl rings are normal to the picrate; in the decamethylferrocene charge-transfer product with 2,3-dichloro-5,6-dicyanoquinone (DDQ)[38] the cyclopentadienyl rings are parallel to the quinone rings; and in the intercalation product of metallocenes with FeOCl,[39] the cyclopentadienyl rings are normal to the layers of the substrate. In some of these the interaction appears to be between the π orbitals of the cyclopentadienyl rings and whatever orbitals are normal to the substrate layers, while in others, the interaction appears to be between the orbitals of the iron atom and the orbitals normal to the layers.

The hydroquinone is hydrogen bonded to two picrates. The hydroxy oxygen O8 is 280.2 (3) pm from the phenoxide oxygen O1, a reasonable distance for hydrogen bonding, and the O8–HO8–O1 angle is 168 (4)°. The O8 oxygen is also 295.9 (4) pm from an oxygen, O7, on a neighboring nitro group, but the O7–HO8–O8 angle is 119 (3)° and the HO8···O7 distance is 248 (4) pm so that this is a much weaker hydrogen bond. Because of the steric hindrance from O1, the ortho nitro groups are not in the plane of the benzene ring. The closest intermolecular approaches, other than the hydrogen–oxygen distances involved in the hydrogen bonding, are between ferrocenophane hydrogens H18 and H19 and a nitro oxygen, O2 (274 and 258 pm, respectively).

Although we consider it unlikely, the presence of the π-orbital interaction between the picrate and the ferrocenophane may be suspected as the cause of the shape of the ferrocenophane and of the short iron–iron distance. This question can be resolved by the determination of the structure of ferrocenophane monocation salts with other anions. We are currently engaged in a search for suitable crystals.

Acknowledgment. We are indebted to Drs. D. Szalda and R. Kirchner for help in using SHELX and to Drs. L.

---

(33) Connelly, N. G.; Dahl, L. F. *J. Am. Chem. Soc.* **1970**, *92*, 7472–7474.

(34) Mason, R.; Mingos, D. M. P. *J. Organomet. Chem.* **1973**, *50*, 53–61.

(35) de Beer, J. A.; Haines, R. J.; Greatrex, R.; van Wyk, J. A. *J. Chem. Soc., Dalton Trans.* **1973**, 2341–2346.

(36) Connelly, N. G.; Dahl, L. F. *J. Am. Chem. Soc.* **1970**, *92*, 7470–7472.

(37) Kaufman, F.; Cowan, D. O. *J. Am. Chem. Soc.* **1970**, *92*, 6198–6204.

(38) Gebert, E.; Reis, A. H., Jr.; Miller, J. S.; Rommelmann, H.; Epstein, A. J. *J. Am. Chem. Soc.* **1982**, *104*, 4403–4410.

(39) Stahl, H. *Inorg. Nucl. Chem. Lett.* **1980**, *16*, 271–276.

K. Hanson and R. Kerber for helpful discussions. This work was supported by the Division of Chemical Sciences, U.S. Department of Energy, Washington, D.C., under Contract No. DE-AC02-76CH00016.

Registry No. I, 87174-38-7.

Supplementary Material Available: Tables of least-squares planes (Table VI), anisotropic thermal factors of non-hydrogen atoms (Table VII), isotropic thermal factors of hydrogen atoms (Table VIII), and observed and calculated structure factors (Table IX) (27 pages). Ordering information is given on any current masthead page.

Organometallic Nitrosyl Chemistry. 20.[1] $(\eta^5\text{-}C_5H_5)W(NO)_2BF_4$, a Versatile Organometallic Electrophile[2]

Peter Legzdins* and David T. Martin

Department of Chemistry, The University of British Columbia, Vancouver, British Columbia, Canada V6T 1Y6

Received June 14, 1983

Treatment of a CH_2Cl_2 solution of $(\eta^5\text{-}C_5H_5)W(NO)_2Cl$ with an equimolar amount of $AgBF_4$ results in the rapid formation of a precipitate of AgCl and a bright green solution of $(\eta^5\text{-}C_5H_5)W(NO)_2BF_4$. This organometallic complex is a thermally unstable, air- and moisture-sensitive species whose characteristic chemistry in CH_2Cl_2 is dominated by its electrophilic nature. Hence, it readily forms adducts of the type $[(\eta^5\text{-}C_5H_5)W(NO)_2L]BF_4$ with Lewis bases, L, capable of good σ donation such as PPh_3 or $P(OPh)_3$. In an analogous manner, the novel complex $[(\eta^5\text{-}C_5H_5)W(NO)_2(\eta^2\text{-}C_8H_{14})]BF_4$ results when $(\eta^5\text{-}C_5H_5)W(NO)_2BF_4$ is exposed to an excess of *cis*-cyclooctene. Other olefins, however, either do not react (e.g., allylbenzene) or undergo dimerization (e.g., 1,1-diphenylethene) or isomerization (e.g., 2,3-dimethyl-1-butene), the latter transformations probably occurring via electrophile-induced formation of incipient carbocations. $(\eta^5\text{-}C_5H_5)W(NO)_2BF_4$ also reacts with CH_2Cl_2-soluble anionic nucleophiles, X^-, to form $(\eta^5\text{-}C_5H_5)W(NO)_2X$ (X = H or Br) products. Of greater interest is the fact that the organometallic nitrosyl reactant is sufficiently electrophilic to cleave the M–C linkages in organic derivatives of the main-group elements (i.e., M = B, Al, or Sn) and so produce some new $(\eta^5\text{-}C_5H_5)W(NO)_2R$ (R = Et, CH_2Ph, or Ph) complexes. This chemistry has also been extended to encompass some of the pentamethylcyclopentadienyl analogues derivable from $(\eta^5\text{-}C_5Me_5)W(NO)_2BF_4$. The physical properties of all new compounds prepared are presented and discussed in relation to possible molecular structures.

Introduction

We recently described the preparation and characterization of several salts of the bimetallic cation $[(\eta^5\text{-}C_5H_5)_2W_2(NO)_4H]^+$.[3] The physical and chemical properties of these compounds indicated that the cation could be viewed as a Lewis acid–base adduct. In this view, the formally 18-electron unit $(\eta^5\text{-}C_5H_5)W(NO)_2H$ provides a pair of electrons from a filled metal- or ligand-centered orbital to a vacant metal-centered orbital of the formally 16-electron unit $(\eta^5\text{-}C_5H_5)W(NO)_2^+$. Further support for the donor–acceptor character of this interaction was provided by the fact that $(\eta^5\text{-}C_5H_5)W(NO)_2H$ also forms adducts with other Lewis acids. On the basis of these studies, it was concluded that $(\eta^5\text{-}C_5H_5)W(NO)_2H$ functions as a fairly weak and soft Lewis base.[3] However, little could be said at that time about the acid component of the bimetallic cation. In this paper we now turn our attention to $(\eta^5\text{-}C_5H_5)W(NO)_2^+$. Specifically, we wish to report its independent synthesis and to present its characteristic chemistry that delineates its electrophilic character.

Experimental Section

All reactions and subsequent manipulations involving organometallic reagents were performed under anaerobic and anhydrous conditions. General procedures routinely employed in these laboratories have been described previously.[3] Gas chromatographic analyses were carried out on a Perkin-Elmer Sigma 4B instrument employing a 8 ft × 0.125 in. column packed with 3% OV-17 on Supelcoport.

Generation of a CH_2Cl_2 Solution of $(\eta^5\text{-}C_5H_5)W(NO)_2BF_4$. Solid $AgBF_4$ (0.40 g, 2.0 mmol) was added to a green solution of $(\eta^5\text{-}C_5H_5)W(NO)_2Cl$[4] (0.69 g, 2.0 mmol) in CH_2Cl (25 mL) that displayed characteristic nitrosyl absorptions at 1733 and 1650 cm^{-1} in its IR spectrum. The reaction mixture was stirred at room temperature for ~20 min, after which time it consisted of a flocculent white precipitate and a darker green supernatant solution. The final mixture was filtered through a medium-porosity frit to obtain a clear, green solution whose IR spectrum exhibited ν_{NO}'s at 1754 and 1674 cm^{-1}. This solution of $(\eta^5\text{-}C_5H_5)W(NO)_2BF_4$ slowly deposited an intractable red-brown solid when stirred at ambient temperature in a prepurified dinitrogen atmosphere, the decomposition being clearly evident after 30 min. The rate of decomposition was markedly enhanced by removal of the solvent in vacuo, an operation which only afforded the red-brown solid. Consequently, the CH_2Cl_2 solutions of $(\eta^5\text{-}C_5H_5)W(NO)_2BF_4$ generated according to this procedure were used immediately for the subsequent chemical transformations described below.

Preparation of $[(\eta^5\text{-}C_5H_5)W(NO)_2L]BF_4$ (L = PPh_3, $P(OPh)_3$, or $\eta^2\text{-}C_8H_{14}$). The CH_2Cl_2 solution of $(\eta^5\text{-}C_5H_5)W(NO)_2BF_4$ was added to a colorless solution of PPh_3 (0.53 g, 2.0 mmol) in CH_2Cl_2 (10 mL). The resulting green solution was stirred briefly and was then permitted to stand for ~10 min, whereupon lustrous green platelets began to crystallize. The crystallization was completed by the addition of Et_2O (50 mL). The solid was collected by filtration, washed with Et_2O (3 × 10 mL), and dried in vacuo (5×10^{-3} mm) at room temperature for 0.5 h to obtain 0.94 g (69% yield) of analytically pure $[(\eta^5\text{-}C_5H_5)W(NO)_2(PPh_3)]BF_4\cdot{}^1/_2CH_2Cl_2$: IR ($CH_2Cl_2$) ν_{NO} 1770 (s), 1694 (vs) cm^{-1}; ^1H NMR ($(CD_3)_2CO$) δ 7.69 (m, 15 H, C_6H_5), 6.54 (d, 5 H, C_5H_5,

---

[1] Part 19: Legzdins, P.; Martin, D. T.; Nurse, C. R.; Wassink, B. *Organometallics* **1983**, *2*, 1238.

[2] For a preliminary account of this work see: Legzdins, P.; Martin, D. T. "Abstracts of Papers", 185th National Meeting of the American Chemical Society, Seattle, WA, March 1983; American Chemical Society: Washington, DC, 1983; INOR 56.

[3] Hames, B. W.; Legzdins, P. *Organometallics* **1982**, *1*, 116.

[4] Hoyano, J. K.; Legzdins, P.; Malito, J. T. *Inorg. Synth.* **1978**, *18*, 126.